Dependence of Glycine CH_2 Stretching Frequencies on Conformation, Ionization State, and Hydrogen Bonding

Sergei V. Bykov, Nataliya S. Myshakina, and Sanford A. Asher*

Department of Chemistry, University of Pittsburgh, Pittsburgh, Pennsylvania 15260

Received: October 18, 2007; In Final Form: February 19, 2008

We experimentally and theoretically examined the conformation, pH, and temperature dependence of the CH_2 stretching frequencies of glycine (gly) in solution and in the crystalline state. To separate the effects of the amine and carboxyl groups on the CH_2 stretching frequencies we examined the Raman spectra of 2,2,2-d_3-ethylamine ($CD_3-CH_2-NH_2$) and 3,3,3-d_3-propionic acid (CD_3-CH_2-COOH) in D_2O. The symmetric (ν_sCH_2) and asymmetric ($\nu_{as}CH_2$) stretching frequencies show a significant dependence on gly conformation. We quantified the relation between the frequency splitting ($\Delta = \nu_{as}CH_2 - \nu_sCH_2$) and the ξ angle which determines the gly conformational geometry. This relation allows us to determine the conformation of gly directly from the Raman spectral frequencies. We observe a large dependence of the ν_sCH_2 and $\nu_{as}CH_2$ frequencies on the ionization state of the amine group, which we demonstrate theoretically results from a negative hyperconjugation between the nitrogen lone pair and the C−H antibonding orbitals. The magnitude of this effect is maximized for C−H bonds trans to the nitrogen lone pair. In contrast, a small dependence of the CH_2 stretching frequencies on the carboxyl group ionization state arises from delocalization of electron density from carboxyl oxygen to C−H bonding orbitals. According to our experimental observations and theoretical calculations the temperature dependence of the ν_sCH_2 and $\nu_{as}CH_2$ of gly is due to the change in the hydrogen-bonding strength of the amine/carboxyl groups to water.

Introduction

Vibrational spectroscopy is a powerful technique to study the conformations of peptides and proteins. Vibrational spectroscopy provides a unique opportunities to study fast protein folding dynamics[1−5] and unordered states of polypeptide chains.[6] Vibrational spectra are highly informative on molecular structure due to the extreme sensitivity of certain vibrational bands or so-called "conformational markers", to the small structural alterations such as bond lengths, dihedral angles, and hydrogen-bonding patterns.

The most commonly used markers for the polypeptide backbone conformation analysis are the amide bands. The amide I band (primarily C═O stretching of the peptide bond) is used for IR spectroscopy secondary structure elucidation.[1,5] The amide II, amide III, and $C_\alpha H$ bending vibrations, observed in Raman spectra, have been shown to be even more valuable for peptide secondary structure analysis.[3,4,7,8] There should be other conformationally sensitive vibrations which can be used to expand the informational context of vibrational spectroscopy.

The CH (or deuterated CD) stretch is a potential candidate for use as a conformational marker to study the secondary structure of polypeptide chains. It has recently been shown theoretically[9,10] that the $C_\alpha H$ ($C_\alpha D$) bond stretching frequency depends on the ψ and φ Ramachandran angles.

CH stretching vibrations have previously been used to determine the structure of small organic molecules. Isolated C−D stretching frequencies have also been used in the conformational analysis of alkylamino chains[11] and monosaccharides.[12] Good correlations have been experimentally found between isolated methyl CH stretching frequencies and HCH angles.[13]

The origin of the CH conformational sensitivity is not well understood. It is generally agreed that the CH stretching frequencies depend almost solely on the C−H bond lengths because these vibrations are essentially decoupled from other vibrations. Previous work has quantified the relationship between CH stretching frequencies and C−H bond lengths in various organic compounds[14,15] This work includes McKean, Bellamy, and others'[16,17] extensive IR spectroscopy studies in 1960s and 1970s which examined the factors influencing CH stretching frequencies.

In the present study we focus our attention on glycine (gly), the smallest amino acid, which has a hydrogen atom instead of a side chain. There is no coupling of the gly CH_2 stretches in proteins and peptides with the CH stretches of the adjacent amino acid residue side chains. In addition, the CH_2 stretches of gly are unaffected by Fermi resonances because of the significant downshift of the CH_2 scissoring vibration. The two CH stretches of the gly CH_2 group couple with each other to form high-frequency asymmetric and low-frequency symmetric CH_2 stretching components, which appear as a doublet in the Raman spectra. The magnitude of the frequency splitting of this doublet depends on the extent of vibrational coupling which in turn is determined by the C−H bond length difference.

The unique flexibility of gly makes it an essential structural element of many proteins, determining protein folding pathways, tertiary structure, and biological function. Gly is frequently found in the turn and loop structures, which play an important role in polypeptide chain collapse during the early stages of folding. Gly accelerates loop formation compared to other amino acids.[18] Gly-rich flexible motifs are often impossible to characterize by X-ray crystallography and 2D NMR.[19] Thus, there

* Corresponding author. Tel.: (412)-624-8570. Fax: (412)-624-0588. E-mail: asher@pitt.edu.

10.1021/jp710136c CCC: $40.75
Published on Web 05/01/2008

is a great need to develop new structural methods to determine the gly residue conformations.

In this article we investigate the gly CH_2 stretching frequency dependence on amino acid conformation and ionization state in order to develop methodologies for the conformational analysis of gly residues in polypeptides and proteins.

Experimental Methods

Sample Preparation. For the pD measurements anhydrous gly (Sigma Chemicals) was dissolved in D_2O (Cambridge Isotope Laboratories Inc). Low and high pD samples were prepared by addition of DCl or NaOD solutions (Sigma Chemicals). 2,2,2-d_3-Ethylamine hydrochloride was obtained from Medical Isotopes Inc., and 3,3,3-d_3-propionic acid was from Cambridge Isotope Laboratories Inc. Crystals of Gly·HCl, Gly·HNO_3, and 3Gly·H_2SO_4 (TGS) were obtained by slow evaporation of water solutions of stoichiometric mixtures of gly and the corresponding acid. All acids were purchased from J. T. Baker Inc. Crystal structures were determined by using X-ray crystallography.

Raman Measurements. All Raman measurements were performed using 488 nm Ar ion laser (Coherent Inc.) excitation. Scattered light was collected using a backscattering geometry, dispersed by a single monochromator, and collected using a Princeton Instruments Spec-10:400B CCD camera (Roper Scientific). A 488 nm holographic notch filter (Kaiser Optical Systems Inc.) was used for Raleigh rejection. Typical accumulation times were ~2 min. A temperature-controlled fused-silica cell (20 mm path length, Starna Cell Inc.) was used for solutions. A custom-made, rotating metal cell was used for solid powder samples to avoid light-induced degradation under continuous irradiation. The powder was pressed into a circular groove cut in the rotating metal cylinder.

Computational Methods

We optimized the geometries and calculated the vibrational frequencies, normal mode compositions, molecular orbital analysis, and charge distributions of a series of gly conformers in neutral and zwitterionic forms. We also performed the calculations for zwitterionic gly hydrogen bonded to one or two water molecules (Figure 1).

All calculations were carried out at the density functional theory (DFT) level of theory[20−22] employing the B3LYP hybrid functional[23−25] and 6-311+G(d,p) basis set. All frequencies were calculated at the harmonic approximation and scaled by 0.98.[26,27] The presence of the solvent water was modeled using the polarizable continuum model (PCM) initially devised by Tomasi and co-workers.[28−30] The PCM calculations were performed using the integral equation formalism model[30] (IEFPCM) and the Bondii's atomic radii. Atomic charges were calculated using the atoms in molecule (AIM) algorithm[31−33] as implemented in Gaussian'98. Orbital occupancies and hybridization analysis of natural local molecular orbitals were obtained through the natural bond orbital (NBO) analysis. All calculations except the AIM charge calculations were performed with the Gaussian'03 calculational package.[34] Normal mode compositions for the calculated vibrational frequencies were obtained from the Gaussian output files employing the GAR2PED program.[35]

Since the primary interest of our study is the conformational dependence of the CH_2 stretching frequencies we constrained the geometry of gly to conformations of interest. We fixed the dihedral angle N1−C3−C6−O9 (defined as ξ) at 0° in the anti and gauche rotamers of neutral gly (Figure 1a) and *eclipsed*-gly$^{\pm}$ (Figure 1b). We fixed ξ at −60° in *twisted*-gly$^{\pm}$. In *staggered*-gly$^{\pm}$ in addition to $\xi = 0°$ we fixed H8−N1−C3−C6 at −60° to prevent its relaxation to more stable *eclipsed*-gly$^{\pm}$. We also studied a series of conformers of neutral gly with the ξ angle fixed at values from 80° to −80°.

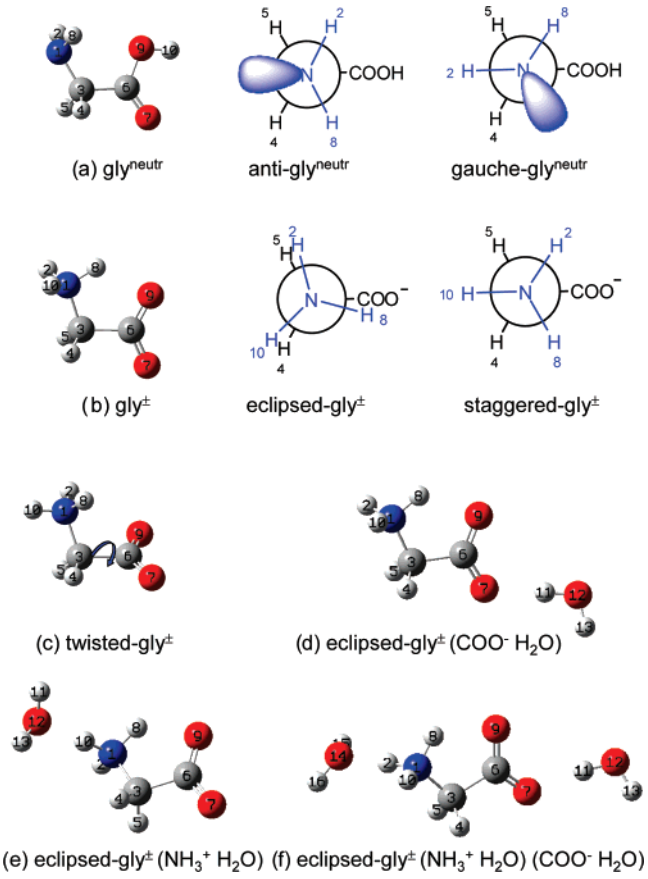

Figure 1. Calculated conformers of gly: (a) anti and gauche rotamers of neutral gly; (b) eclipsed and staggered rotamers of zwitterionic gly; (c) nonplanar conformer ($\xi = -60°$) of zwitterionic gly; (d) eclipsed zwitterionic gly hydrogen bonded to the donor water molecule; (e) eclipsed zwitterionic gly hydrogen bonded to the acceptor water molecule; (f) eclipsed zwitterionic gly hydrogen bonded simultaneously to the acceptor and donor water molecules. All conformers except (c) are planar $\xi = 0°$.

Experimental Results

Conformational Dependence of the CH_2 Stretching Frequencies on Carboxyl Group Orientation of Gly in the Solid State. We investigated the structures of gly found in the Cambridge Structural Database (CSD):

(1) Gly hydrochloride (Gly·HCl). In this crystal all heavy atoms lie almost in the same plane.[36]

(2) Gly nitrate (Gly·HNO_3). Here gly is bent.[37]

(3) Triglycine sulfate (3Gly·H_2SO_4), TGS. In this crystal structure two gly molecules have geometries close to planar while one gly molecule is bent.[38]

In these structures the amine groups are protonated ($-NH_3^+$). Thus, rotation about the N−C bond should not significantly affect the CH_2 stretching frequencies.

There is a remarkable difference in the frequencies and the frequency splitting between the CH_2 symmetric ($\nu_s CH_2$) and asymmetric ($\nu_{as} CH_2$) stretching frequencies for these three samples. The Raman spectrum of crystalline Gly·HCl shows the symmetric and asymmetric stretching bands at $\nu_s CH_2 = 2962$ cm^{-1} and $\nu_{as} CH_2 = 2996$ cm^{-1}, with a splitting Δ of ~34 cm^{-1}.

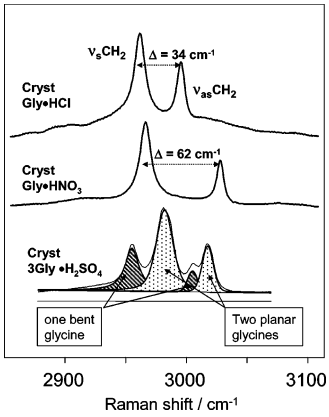

Figure 2. Raman spectra of the CH stretching region of crystalline gly hydrochloride (Gly·HCl), crystalline gly nitrate (Gly·HNO_3), and crystalline triglycine sulfate or TGS (3Gly·H_2SO_4).

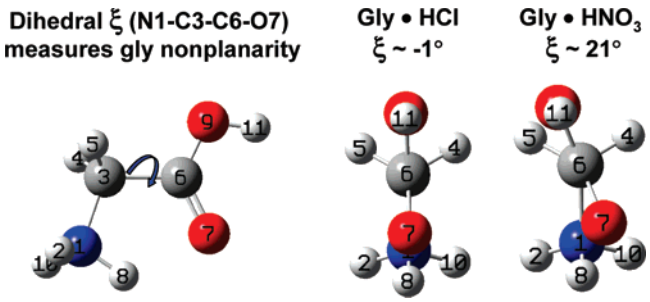

Figure 3. Dihedral angle ξ measures the planarity of the gly molecule. If $\xi \sim 0°$, the molecule is planar and the C−H bonds are symmetric with respect to the carboxyl group plane, as in case of Gly·HCl. In Gly·HNO_3 the carboxyl is rotated ~21° with respect to the N1−C3 bond making the C−H bonds nonequivalent.

Crystalline Gly·HNO_3 has a much larger splitting, $\Delta \sim 62$ cm^{-1} between the $\nu_s CH_2 = 2966$ cm^{-1} and $\nu_{as} CH_2 = 3028$ cm^{-1} bands, mainly due to the upshift of the $\nu_{as} CH_2$. TGS has three nonequivalent gly in the crystal unit cell. In TGS we observe two different doublets of $\nu_s CH_2$ and $\nu_{as} CH_2$.

X-ray crystallographic data shows (Figure 3) that in Gly·HCl crystals all heavy atoms (N−C−COO) lie almost in the same plane and the two C−H bonds are symmetrically disposed about this plane. The dihedral angel ξ, defined by atoms N−C−C−$O_{cis\ to\ N}$ (since the carboxyl group has two oxygens, ξ is defined by the one which is the closest (cis) to the nitrogen). The ξ angle indicates the deviation of gly from the planar conformation through rotation around the C−C bond. When $\xi = 0°$ all heavy atoms in the gly molecule lie in the same plane (Figure 3). In contrast, the −COOH group of the Gly·HNO_3 crystal is rotated such that $\xi \sim 21°$. In this case the C−H bonds are not symmetrically disposed on both sides of the COO plane, which results in greater splitting between the $\nu_s CH_2$ and $\nu_{as} CH_2$ frequencies.

In TGS crystals, two of the gly molecules are almost planar ($\xi = 4°$ and 5°), while the third one is bent $\xi \sim 21°$. Thus, we assign the more intense, less split doublet (2982 and 3017 cm^{-1}) to the two planar gly molecules and the less intense more split doublet (2956 and 3005 cm^{-1}) to the third gly.

pD and Temperature Dependences of the CH_2 Stretching Frequencies of Gly in Solution. We investigated the influence of the ionization state of the carboxyl and amine groups on the CH_2 stretching vibrations. Deuteration of the amine in gly molecule significantly downshifts the N−D stretches which removes overlap or coupling between C−H and N−D stretches and simplifies the interpretation of the Raman spectra.

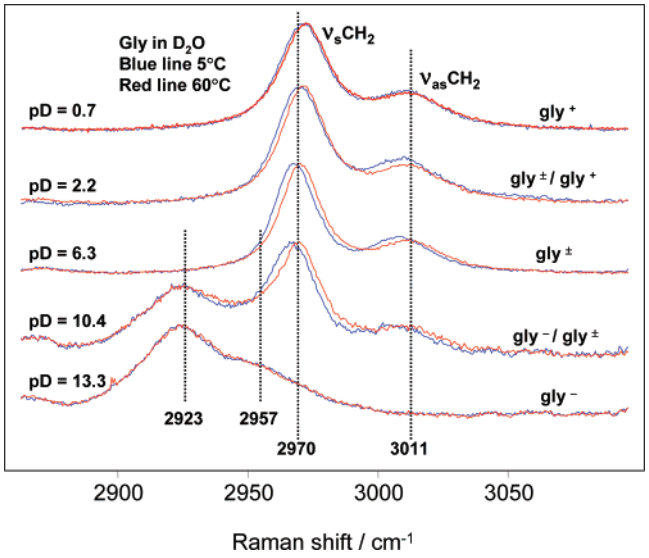

Figure 4. 488 nm excitation Raman spectra of gly solution in D_2O at pD = 0.7, 2.2, 6.3, 10.4, and 13.3. For each solution spectra were accumulated at two temperatures, 5 and 60 °C.

TABLE 1: Temperature Dependence of the Raman CH_2 Stretching Frequencies of Gly in D_2O

solution	T °C	$\nu_s CH_2$/ cm^{-1}	$\Delta\nu$/ ΔT sym	$\nu_{as} CH_2$/ cm^{-1}	$\Delta\nu$/ ΔT asym
D_2O pD = 0.7	5	2971.2	0.016	3011.2	0.025
	60	2972.1		3012.6	
D_2O pD = 2.2	5	2969.9	0.027	3009.3	0.055
	60	2971.4		3012.3	
D_2O pD = 6.3	5	2968.1	0.038	3008.6	0.064
	60	2970.2		3012.1	
D_2O pD = 13.3	5				
	60	2923.1	0	2956.8	0

Figure 4 shows the 488 nm Raman spectra of gly in D_2O at various pD values at 5 and 60 °C. At low pD values gly is cationic $D_3N^+-CH_2-COOD$ (gly^+), whereas at pD values close to neutral gly is zwitterionic $D_3N^+-CH_2-COO^-$ ($gly^\pm$), and at high pD values gly is anionic $D_2N-CH_2-COO^-$ (gly^-).

pD Dependence. For the low pD (gly^+) and neutral pD values ($gly^\pm$) the CH_2 stretching region Raman spectra are very similar, indicating that the ionization state of the carboxyl group has little effect on the CH_2 group stretching frequencies. The CH_2 symmetric stretch is at ~2970 cm^{-1} and is ~4 times more intense than the CH_2 asymmetric stretch at ~3010 cm^{-1}.

For pD values close to or above the pK_a value of the gly amine group (pD = 9.8) a peak appears at lower frequency ~2920 cm^{-1}, which must be due to C−H bond weakening due to interaction with the lone pair of the unprotonated amine group ($-ND_2$), as discussed in detail below.

The frequency splitting between $\nu_s CH_2$ and $\nu_{as} CH_2$ is ~41 cm^{-1} for gly^+ and $gly^\pm$, whereas for gly^- it is smaller ($\Delta \sim 34$ cm^{-1}).

Thus, the C−H bonds stretching frequencies depend only on the ionization state of the terminal amine with a little influence of the ionization state of the carboxyl.

Temperature Dependence. Figure 4 and Table 1 indicate the temperature dependence of the CH_2 stretching frequencies of gly in D_2O.

There is a significant temperature dependence of the symmetric and asymmetric CH_2 stretching frequencies on pD. Temperature-induced frequency shifts are larger at neutral pD

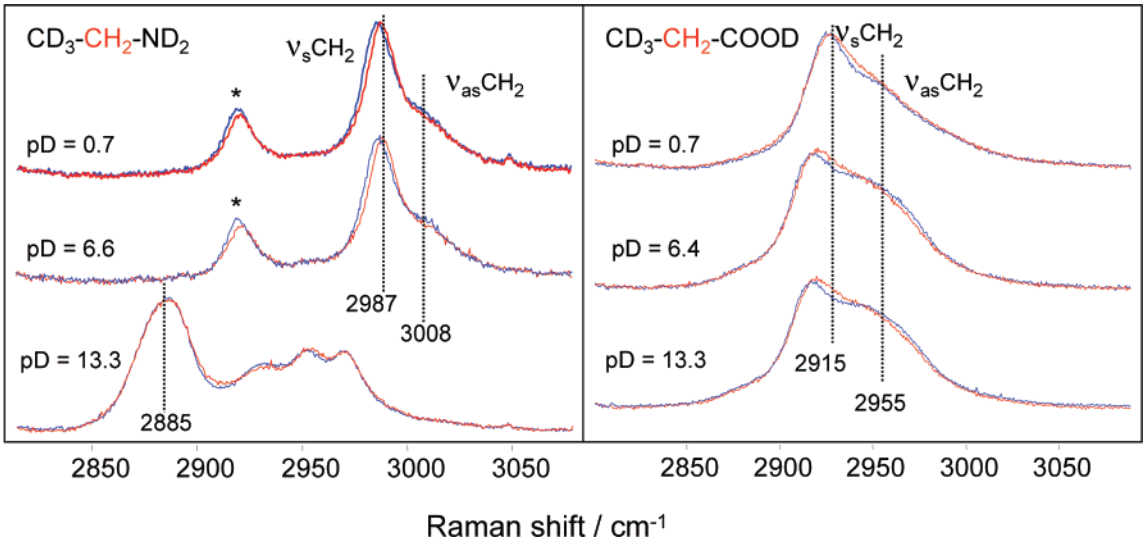

Figure 5. CH_2 stretching region of the Raman spectra of the 2,2,2-d_3-ethylamine and 3,3,3-d_3-propionic acid in D_2O at different pD values at 5 (blue curve) and 60 °C (red curve). The band marked with (∗) at 2918 cm^{-1} in 2,2,2-d_3-ethylamine is most likely due to Fermi resonance of the ν_sCH_2 with the overtone of the CH_2 scissoring. The splitting between symmetric and asymmetric CH_2 stretches in $CD_3-CH_2-ND_3^+$ at pD = 0.7 and 6.6 is unusually small, ∼19 cm^{-1} (an additional indication that ν_sCH_2 is upshifted due to Fermi resonance). In gly and propionic acid CH_2 scissoring is at a significantly lower frequency than in ethylamine which removes the condition for Fermi resonance.

than at high or low pD values. At pD = 13.3 the broad low-frequency doublet is essentially temperature independent.

The stretching frequencies of gly methylene are affected by both the amine and carboxyl groups. In order to characterize the impact of the amine and carboxylic groups separately we investigated the CH_2 stretching frequencies of 2,2,2-d_3-ethylamine ($CD_3-CH_2-NH_2$) and 3,3,3-d_3-propionic acid (CD_3-CH_2-COOH) in D_2O at different pD values and temperatures.

pD and Temperature Dependence of the CH_2 Stretching Vibrations of CD_3-CH_2-COOD and $CD_3-CH_2-ND_2$. *pD Dependence.* In $CD_3-CH_2-ND_2$ and CD_3-CH_2-COOD, the CH_2 is affected by changes in the ionization state of either the amine or carboxylic groups.

Figure 5 shows the CH_2 stretching region of the Raman spectra of $CD_3-CH_2-ND_2$ and CD_3-CH_2-COOD in D_2O. At low and neutral pD values 2,2,2-d_3-ethylamine is in its cationic form ($CD_3-CH_2-ND_3^+$). The ν_sCH_2 and $\nu_{as}CH_2$ frequencies are 2987 and 3008 cm^{-1}, respectively. At high pD values 2,2,2-d_3-ethylamine is in its neutral form ($CD_3-CH_2-ND_2$) where the nitrogen possesses a lone pair of electrons. As in gly, the adjacent ND_2 group significantly downshifts the CH_2 stretching vibrations.

The Raman spectrum of the 2,2,2-d_3-ethylamine at pD = 13.3 consists of four bands in the CH_2 stretching region which are due to the free rotation about the C−N bond and presence of both gauche and anti rotamers. The gauche form is slightly more stable (∼0.3 kcal/mol), and the gauche−anti rotational barrier is about 2 kcal/mol for the vapor phase.[39] The assignment of the high pD spectrum will be given later in the discussion after getting additional information from theoretical calculations.

The 3,3,3-d_3-propionic acid CH_2 stretching vibrations (ν_sCH_2 ∼ 2915 cm^{-1} and $\nu_{as}CH_2$ ∼ 2955 cm^{-1}) show a weak frequency dependence on solution pD. At neutral and high pD, the anionic $CD_3-CH_2-COO^-$ CH_2 stretching bands are somewhat broader than are those of the protonated species at low pD.

Temperature Dependence. High pD neutral 2,2,2-d_3-ethylamine ($CD_3-CH_2-ND_2$) shows no CH_2 stretching temperature dependence (Figure 5). In the cationic form (at low and neutral pD values) the CH_2 symmetric stretches upshift with temperature similar to that of the CH_2 symmetric stretch of $gly^{\pm}$, whereas the temperature shift of the CH_2 asymmetric stretch is 2-fold smaller. Table 2 shows the CH_2 stretching frequencies and their temperature dependence.

TABLE 2: Temperature Dependence of the CH_2 ν_s and ν_{as} of 2,2,2-d_3-Ethylamine in D_2O

pD	T °C	ν_sCH_2/cm^{-1}	$\Delta\nu/\Delta T$ sym	$\nu_{as}CH_2/cm^{-1}$	$\Delta\nu/\Delta T$ asym
0.7	5	2985.7	0.033	3006.3	0.033
	60	2987.5		3008.3	
6.6	5	2986.1	0.033	3007.5	0.022
	60	2987.9		3008.7	

The temperature-induced CH_2 stretching frequency shifts in 2,2,2-d_3-ethylamine are similar to those of zwitterionic gly (compare Tables 1 and 2). 3,3,3-d_3-Propionic acid, in contrast, shows little temperature dependence of the CH_2 stretching frequencies for any solution pD values. Thus, we can conclude that the amine group dominates the temperature dependence of the CH_2 stretching frequencies in gly.

pD and Temperature Dependence of the CD_3 Stretching Frequency in CD_3-CH_2-COOD and $CD_3-CH_2-ND_2$. Deuteration of the methyl group in $CD_3-CH_2-ND_2$ and CD_3-CH_2-COOD separates the originally overlapping methylene and methyl stretching vibrations, allowing us to unambiguously observe these vibrations in different solution conditions.

Figure 6 shows the CD_3 stretching region for 2,2,2-d_3-ethylamine and 3,3,3-d_3-propionic acid at different pD values and temperatures. For both compounds, the CD_3 stretching frequencies depend on the carboxyl or amine ionization states.

At pD = 0.7 and pD = 6.6 the 2,2,2-d_3-ethylamine cation ($CD_3-CH_2-ND_3^+$) shows ν_sCD_3 frequencies of 2135 cm^{-1} and $\nu_{as}CD_3$ frequencies of 2250 cm^{-1} (Figure 6). In contrast, at pD = 13.3 the ν_sCD_3 vibration of neutral $CD_3-CH_2-ND_2$ splits in two bands. One remains near ∼2135 cm^{-1}, whereas the other downshifts 52 cm^{-1} to 2083 cm^{-1}. The $\nu_{as}CD_3$ of the neutral form downshifts ∼14 cm^{-1} to 2236 cm^{-1} and broadens. For 3,3,3-d_3-propionic acid the $\nu_{as}CD_3$ downshifts ∼8 cm^{-1} (from 2245 to 2237 cm^{-1}) as the carboxylic acid (pD = 0.7) becomes a carboxylate anion (pD = 6.4 and 13.3).

From these data we conclude that the CD_3 stretches in $CD_3-CH_2-ND_2$ and CD_3-CH_2-COOD show the pD-induced frequency shifts of about the same magnitude as do the CH_2 stretches, despite the fact that the CD_3 group is not directly

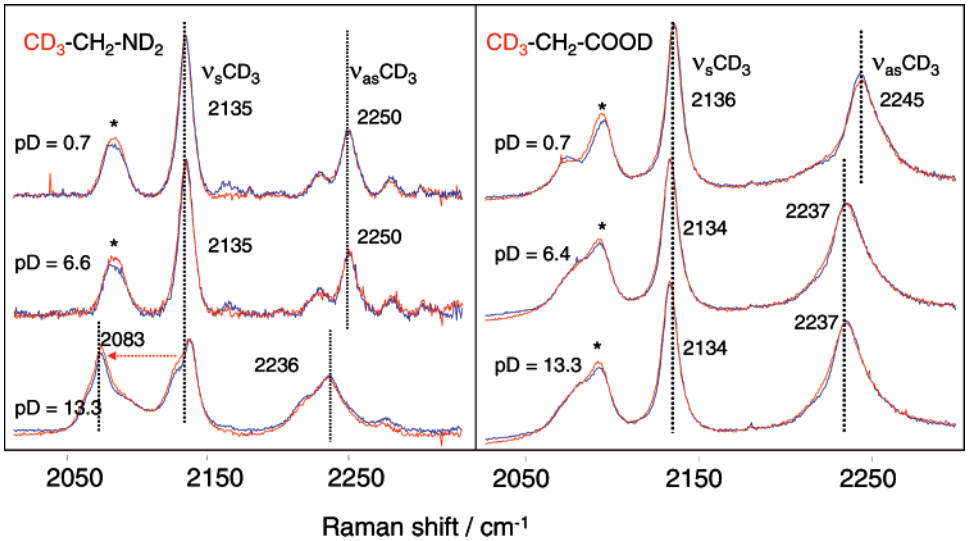

Figure 6. CD_3 stretching region of the 2,2,2-d_3-ethylamine and 3,3,3-d_3-propionic acid in D_2O at different pD values at 5 (blue curve) and 60 °C (red curve). CD_3 stretches show a clear dependence on the ionization state of the amine and carboxylic groups even though the CD_3 group is not directly linked to the carboxyl or amine groups. Frequencies of the ν_sCD_3 and $\nu_{as}CD_3$ for both 2,2,2-d_3-ethylamine and 3,3,3-d_3-propionic acid do not show any temperature dependence at any pD values. The band marked by (∗) is an overtone of CD_3 asymmetric bending ($2\delta_{asym}$ CD_3) enhanced due to Fermi resonance with intense CD_3 symmetric stretch (ref 40).

attached to the ND_2 or COOD groups. It should be noted, however, that although the CD_3 group is not directly bound to the amine or carboxyl group, it is very close to them, in their equilibrium conformations. The CD_3 deuterium atoms are closer to the carbonyl oxygen or nitrogen lone pairs than are the CH_2 group hydrogens.

In contrast to CH_2 stretching vibrations the CD_3 stretches show no temperature dependence for any pD value for both 2,2,2-d_3-ethylamine and 3,3,3-d_3-propionic acid. In both these compounds the CH_2 group is directly linked to amine or carboxyl groups by a σ-bond, whereas the CD_3 group is only spatially close. This indicates that in order to show a CH_2 stretching frequency temperature dependence the CH_2 group must be directly linked to the amine or carboxyl group.

Theoretical Calculations

Effect of Carboxyl Group Orientation on the CH_2 Stretching Frequencies. The experimental results indicate a dependence of the CH_2 stretching frequencies on carboxyl group orientations. Although in real crystals the range of available conformations is limited because gly prefers to be in planar conformations where ξ is small,[41] theoretical calculations allow us to explore a much broader range of conformations. Thus, we theoretically modeled the conformational dependence of CH_2 vibrations frequencies upon the ξ angle for neutral gly. We fixed the orientation of $-NH_2$ group with respect to the CH_2 group to rule out any possible impact of nitrogen lone pair orientation.

As expected from experiments, our theoretical results show that the $\nu_{as}CH_2$ and ν_sCH_2 frequencies significantly depend on ξ (Figure 7A), and these frequencies correlate with the C−H bond lengths (Figure 7B).

For $\xi = 0°$ the C−H bonds symmetrically arrange with respect to the carboxyl group plane and have identical bond lengths (Figure 7B). This results in the minimum calculated frequency splitting between the $\nu_{as}CH_2$ and ν_sCH_2 coordinates ($\Delta_{0°,calc} = 33$ cm^{-1}). At $\xi = \pm 31°$ one of the C−H bonds is almost perpendicular to the carboxyl plane, whereas the other lies within the COO plane. These conformations have the maximal frequency splitting between the ν_s and ν_{as} CH_2 stretching frequencies and the largest differences in C−H bond lengths. At $\xi = \pm 81°$ the ν_sCH_2 and $\nu_{as}CH_2$ frequencies are at their maximum values, both C3−H4 and C3−H5 bonds have their shortest bond lengths, and both lie almost within the COO plane (Figure 7, top). It should also be noted that calculated CH_2 stretching frequencies and frequency splitting in gly rotamers with the OH group in cis and trans position to the amine group are essentially identical.

The normal mode composition indicates that the extent of coupling between the two C−H stretching vibrations depends on the difference in C−H bond lengths. For planar gly ($\xi = 0°$) with equivalent C−H bonds, both C−H stretching vibrations contribute equally to symmetrical and asymmetrical components of CH_2 stretching (Figure 7C). At $\xi = \pm 31°$, where the C−H bond length difference is the largest, the coupling is smallest, and each calculated C−H stretching mode is an almost local vibration. The longer the C−H bond length, the more it contributes to the low-frequency symmetric vibration and vice versa.

Our experimental data and our theoretical modeling show that the proximity of the C−H bond to the carboxyl group oxygen results in significant upshift of the corresponding CH stretching frequencies due to C−H bond shortening.

As shown above, the carboxyl group orientation affects the C−H bond length. To study the carboxyl group orientation effect on the gly electronic structure, we calculated the AIM charge distributions for the $\xi = 0°$, $\xi = 31°$, and $\xi = 81°$ gly conformers. The calculated charge distributions indicate that the C−H bond length decrease results from transfer of electron density from the carboxyl group oxygen to the nearest methylene hydrogen which decreases the oxygen negative charge and decreases the hydrogen positive charge. The magnitude of this effect depends on the distance between the C═O and C−H bonds. At $\xi = 0°$, where both hydrogens are equidistant from the COOH plane, the two methylene hydrogens have equal charge (Table 3). At $\xi = 81°$ both hydrogens are closer to the COOH plane than in the $\xi = 0°$ conformer.

Consequently, the hydrogens will have similar, less positive charges than for the $\xi = 0°$ conformer. In addition, the negative charges on both oxygens are decreased compared to the $\xi = 0°$ conformer. In the $\xi = 31°$ conformer, the hydrogen atom of

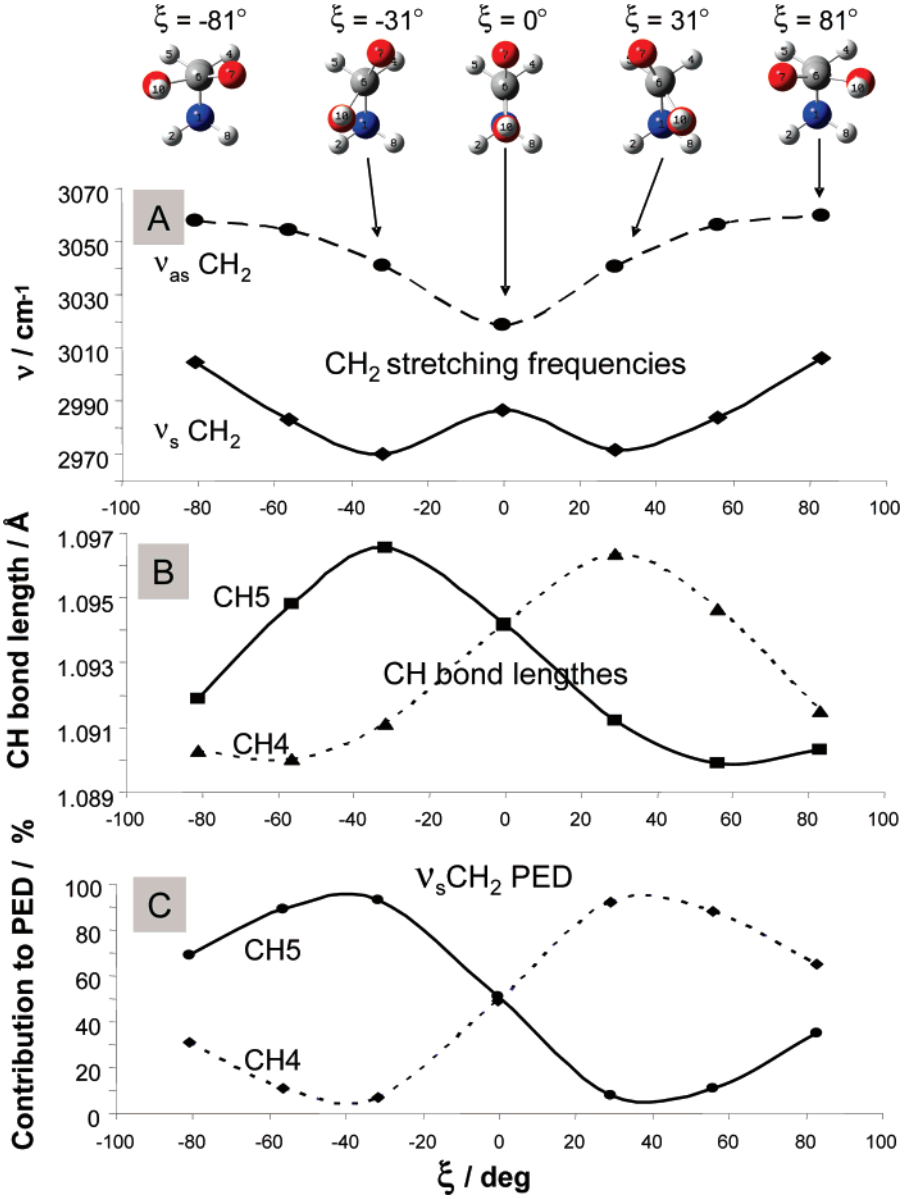

Figure 7. Calculated ξ angular dependence of (A) gly CH_2 stretching frequencies, (B) C−H bond lengths, and (C) normal mode composition (%) of CH_2 symmetric stretch. Frequencies are scaled to 0.98.

TABLE 3: AIM Charge Distributions for Selected ξ Conformations

	$\xi = 0°$	$\xi = 81°$	$\xi = 31°$
N1	−1.014	−1.001	−1.012
H2	0.366	0.368	0.369
C3	0.365	0.367	0.366
H4	0.052	0.044	0.047
H5	0.052	0.041	0.051
C6	1.503	1.493	1.501
O7	−1.208	−1.199	−1.203
H8	0.366	0.370	0.365
O9	−1.122	−1.121	−1.124
H10	0.641	0.064	0.641

the C−H bond closest to the COOH plane has less positive charge than does the other, while the negative charge on the oxygen decreases.

Theoretical Modeling of the pD Dependence of CH_2 Stretching Frequency: Effect of the Amine and Carboxyl Ionization States and Orientations. We calculated the geometry, electronic structure properties, vibrational frequencies, and normal mode compositions for a series of gly conformers in neutral and zwitterionic forms in solution. Both neutral and zwitterionic forms were calculated in an implicit solvent with the dielectric constant of water modeled by PCM. PCM was employed to both stabilize the zwitterion, which is unstable in gas-phase calculations, and to account for the macroscopic effects of water.

Amine Group Effect. The nitrogen lone pair impact on the C−H stretching frequencies of organic compounds has been referred to as either the "trans effect of lone pair", "negative hyperconjugation", or "the Bohlmann effect".[16,42] C−H bonds within the same CH_3 or CH_2 groups linked to an atom carrying a lone pair of electrons often have different lengths.[43] Some C−H bonds are substantially longer which results in large frequency downshifts (up to 150 cm^{-1}). This phenomenon is especially prominent in cases with nitrogen or oxygen lone pair electrons. The specific influence of the lone pair is confirmed by the disappearance of C−H bond lengthening when the lone pair was removed.

It is generally agreed that the trans C−H bond weakening occurs because of partial transfer of the lone pair electrons to the vacant σ^* orbital of the C−H bond.[44] The stretching

TABLE 4: Calculated C−H Bond Lengths, C−H Stretching Frequencies, Normal Mode Compositions, and AIM Charge Distributions for Neutral, Zwitterionic Gly Conformer, and the Hydrogen-Bonded Zwitterionic Gly−Water Conformers[a]

		gly^{neut}		gly$^{\pm}$			gly$^{\pm}$−water complexes		
		anti-gly^{neut}	*gauche*-gly^{neut}	*eclipsed*-gly$^{\pm}$	*staggered*-gly$^{\pm}$	*twisted*-gly$^{\pm}$ $\xi = -60°$	*eclipsed*-gly$^{\pm}$ NH_3 H_2O	*eclipsed*-gly$^{\pm}$ COO^- H_2O	*eclipsed*-gly$^{\pm}$ NH_3 H_2O, COO^- H_2O
l(C−H), Å	C3−H4	1.096	1.095	1.090	1.091	1.089	1.091	1.090	1.090
	C3−H5	1.096	1.101	1.090	1.091	1.091	1.090	1.090	1.091
freq, cm^{-1} *a*	$\nu_s CH_2$	2962	2902	3015	3007	3008	3011	3017	3012
	$\nu_{as} CH_2$	2995	2983	3069	3063	3074	3063	3073	3065
PED, %	$\nu_s CH_2$	C−H5 s (51)	C−H5 s (97)	C−H4 s (50)	C−H5 s (50)	C−H5 s (67)	C−H4 s (55)	C−H4 s (52)	C−H4 s (56)
		C−H4 s (48)	C−H4 s (3)	C−H5 s (48)	C−H4 s (49)	C−H4 s (33)	C−H5 s (44)	C−H5 s (47)	C−H5 s (44)
	$\nu_{as} CH_2$	C−H4 s (51)	C−H4 s (97)	C−H5 s (51)	C−H4 s (50)	C−H4 s (66)	C−H5 s(55)	C−H5 s(52)	C−H5 s(56)
		C−H5 s (48)	C−H5 s (3)	C−H4 s (49)	C−H5 s (49)	C−H5 s (33)	C−H4 s (44)	C−H4 s (48)	C−H4 s (44)
AIM charges	N1	−1.013	−1.003	−0.980	−0.962	−0.959	−1.010	−0.979	−1.010
	H2	0.364	0.364	0.468	0.473	0.473	0.455	0.469	0.504
	C3	0.359	0.348	0.244	0.249	0.261	0.250	0.247	0.253
	H4	0.052	0.055	0.083	0.080	0.070	0.073	0.086	0.079
	H5	0.052	0.034	0.083	0.080	0.076	0.076	0.086	0.076
	C6	1.508	1.523	1.654	1.660	1.647	1.648	1.655	1.649
	O7	−1.204	−1.204	−1.257	−1.263	−1.254	−1.261	−1.235	−1.239
	H8	0.364	0.361	0.482	0.472	0.473	0.469	0.481	0.468
	O9	−1.134	−1.128	−1.241	−1.256	−1.257	−1.246	−1.231	−1.236
	H10	0.642	0.641	0.468	0.469	0.473	0.502	0.470	0.456

[a] Frequencies are scaled by 0.98.

frequency of the C−H bond trans to the lone pair is significantly decreased compared to that of the gauche C−H bond.[45,46] It should be noted that "lone pair trans effect" is quite general, also occurring for OH, NH, etc.[46]

Transfer of electronic density to a σ^* orbital is expected to be particularly favored when the acceptor orbital presents a smooth, nodeless character in the region of the donor orbital as do σ^*C−H orbitals. The best donor orbital for such interaction would be a diffuse lone pair nonbonding orbital, such as the nitrogen lone pair. From the shapes of these orbitals, simple consideration suggests that the n−σ^* interaction is optimized in a linear "end-on" arrangement. Thus, the strongest n−σ^* interactions would occur for the C−H bond trans to the lone pair, since this particular orientation gives a linear arrangement of the nitrogen lone pair relative to the C−H antibonding orbital (Figure 1).

We examined the effect of the nitrogen lone pair on two conformations of neutral gly with different orientations of the CH_2 group relative to the NH_2 group (Figure 1a). In *anti*-gly^{neut} the nitrogen lone pair is gauche to both C−H bonds, where both C−H bonds are approximately equidistant from the lone pair. In contrast, in *gauche*-gly^{neut} one of C−H bond (C3−H4) is gauche to the nitrogen lone pair, while the other (C3−H5) is trans. In zwitterionic gly such orientations are not differentiated because of the lack of the nitrogen lone pair.

For neutral gly our calculations show that *anti*-gly^{neut} has equivalent C−H bonds, whereas in *gauche*-gly^{neut} the C3−H5 bond trans to the nitrogen sp^3 lone pair orbital is significantly elongated, while the other bond is slightly contracted compared to *anti*-gly^{neut} (Table 4). In zwitterionic gly both C−H bonds have equal length. The zwitterionic C−H bonds shorten because of the proximity of the positively charged NH_3^+ group.

The C−H stretching frequencies differ between *anti*-gly^{neut} and *gauche*-gly^{neut}. In *anti*-gly^{neut} the $\nu_s CH_2$ is calculated at 2962 cm^{-1}, whereas in *gauche*-gly^{neut} this vibration downshifts by 60 cm^{-1} compared to that in *anti*-gly^{neut}. The frequency splitting between the symmetrical and asymmetrical components of CH_2 also differs in these structures. In *anti*-gly^{neut}, where both C−H bonds are equal, the split is 33 cm^{-1}, whereas in *gauche*-gly^{neut} the split is a much larger 81 cm^{-1} (Table 4). Our Raman spectra of gly at pD = 13.3 show a 34 cm^{-1} splitting between the two CH_2 stretching peaks which agrees well with the frequencies calculated for *anti*-gly^{neut}. This suggests that at high pH gly exists mainly in the *anti*-gly^{neut} conformation. However, the breadth of both CH_2 stretching bands indicates the existence of additional conformations in solution.

C−H bond length changes impact the coupling between the CH_2 stretching vibrations (Table 4). In *anti*-gly^{neut} both C−H bonds contribute equally to the asymmetric and symmetric components. In contrast, in *gauche*-gly^{neut} the two C−H vibrations are uncoupled. The high-frequency vibration is almost a pure stretch of the shorter C−H bond, whereas the low-frequency band is almost a pure stretch of the longer C−H bond.

In zwitterion gly the C−H bonds have the same length but are shorter than in *anti*-gly^{neut}. Consequently, both symmetric and asymmetric stretches of CH_2 occur at higher frequencies (Table 4) The calculated zwitterion CH_2 54 cm^{-1} frequency splitting is larger than for the *anti*-gly^{neut} conformer. We also observe a larger frequency splitting of the CH_2 stretching vibrations at lower pD than at higher pD.

The charge distribution on the CH_2 group (Table 4) indicates that in the zwitterion each C−H bond is more polar than in the neutral form. This increased bond polarity results from the nitrogen negative inductive effect, which shortens the zwitterionic C−H bonds. In *anti*-gly^{neut}, the C−H bond lengths and charges on both methylene hydrogens are equal. In *gauche*-gly^{neut}, different bond lengths and charge distributions occur. The longest C−H bond hydrogen atom is less positive than the other, whereas the positive charge is almost equal to that in *anti*-gly^{neut}. In *gauche*-gly^{neut} the decreased hydrogen positive charge indicates an increased electronic density transferred from the nitrogen lone pair, since the nitrogen negative charge is decreased compared to that in *anti*-gly^{neut}. The correlation of an increased electronic density with a bond length elongation indicates that the electronic density was accepted by an orbital with non- or antibonding character; the NBO analysis shows an increased occupancy of the C−H σ^* MO (Table 5). This interaction elongates the corresponding C−H bond resulting in

TABLE 5: NBO Calculated Occupancies of Selected Molecular Orbitals of Methylene, Amino, and Carboxyl Groups in Neutral and Zwitterionic Gly Conformers

			gly^{neut}		gly$^{\pm}$			gly$^{\pm}$−water complexes		
			anti-gly^{neut}	*gauche*-gly^{neut}	*eclipsed*-gly$^{\pm}$	*staggered*-gly$^{\pm}$	*twisted*-gly$^{\pm}$ $\xi = -60°$	*eclipsed*-gly$^{\pm}$ NH_3 H_2O	*eclipsed*-gly$^{\pm}$ COO^- H_2O	*eclipsed*-gly$^{\pm}$ NH_3 H_2O, COO^- H_2O
MO occupancy	σ	C−H4	1.964	1.963	1.978	1.976	1.985	1.978	1.978	1.978
		C−H5	1.964	1.969	1.978	1.976	1.979	1.978	1.978	1.978
	σ*	C−H4	0.0157	0.0139	0.0083	0.0096	0.0107	0.0094	0.0083	0.0084
		C−H5	0.0157	0.0287	0.0083	0.0096	0.0096	0.0085	0.0083	0.0094
		LP N	1.950	1.958				N/A		
	COO^-	LP_2 O7	1.863	1.864	1.884	1.885	1.897	1.886	1.874	1.875
		LP_3 O9	N/A		1.631	1.616	1.613	1.629	1.825	1.612
		LP_2 O9	1.799	1.797	1.872	1.892	1.893	1.876	1.869	1.873
		BD CO7	1.996	1.996	1.996	1.996	1.988	1.996	1.832	1.993
	NH_3^+	BD N−H2	N/A		1.994	1.993	1.993	1.994	1.994	1.993
		BD N−H8	N/A		1.993	1.994	1.994	1.993	1.993	1.993
		BD N−H10	N/A		1.994	1.994	1.993	1.993	1.994	1.994

a downshift of the C−H stretching frequency in the gly anion compared to the zwitterion or cation, where the lone pair is removed by protonation. This explains the strong dependence of C−H stretching frequencies on the ionization state of the gly amino group.

Effect of the Carboxyl Group in Zwitterionic Gly. Comparison of the solution gly Raman spectra measured at pD = 0.7 (cationic form) and pD = 6.3 (zwitterionic form) show that the carboxyl group ionization does not significantly affect the CH stretching vibrations. The frequency shift of both C−H stretching vibrations does not exceed 3 cm^{-1} (see Table 1). The charge distribution calculated for the $\xi = 0°$ (staggered) and $\xi = -60°$ (twisted) conformations of gly zwitterion (Table 4) indicates that the C−H bond length decrease is caused by redistribution of electronic density from the C═O bond lying in the same plane with the C−H bond. Analysis of the molecular orbital occupancy (Table 5) shows a significantly increased occupancy of the bonding orbital of the short C3−H4 bond and a decreased O7 lone pair molecular orbital occupancy. The 0.002 Å bond length difference between the C−H bonds of *twisted*-gly$^{\pm}$ prevents coupling between the two CH stretches. PED indicates that two CH stretching frequencies calculated for *twisted*-gly$^{\pm}$ result from almost pure vibrations of the individual C−H bonds, whereas in *staggered*-gly$^{\pm}$ the CH stretching motions are coupled into symmetric and asymmetric vibrations (Table 4). In *twisted*-gly$^{\pm}$ the C−H bond contraction results in an 11 cm^{-1} upshift of the high-frequency CH stretch, while the low-frequency CH stretch is equal to that in *staggered*-gly$^{\pm}$.

Effect of Hydrogen Bonding to Amine and Carboxyl Groups on the CH (CD) Stretching Frequencies of Glycine, Deuterated Ethylamine, and Propionic Acid. As shown above the electronic configuration of the nitrogen atom and spatial orientation of the carboxyl group have a large impact on the neighboring CH_2 bond lengths and stretching frequencies. Hydrogen bonding to $-NH_3^+/-NH_2$ and $-COOH/-COO^-$ of gly affects the electronic configurations of these groups which, in turn, change the CH_2 bond strengths, which shift the CH_2 stretching frequencies.

To examine the effect of water hydrogen bonding on the C−H frequencies, we calculated the geometries and electronic properties of gly zwitterion ($\xi = 0°$), the zwitterion with water attached to the NH_3^+ group, and the zwitterion with water attached to the COO^- site. We also examined gly zwitterion with waters attached to both NH_3^+ and COO^-.

Water hydrogen bonding to the gly $-COO^-$ terminus does not change the C−H bond lengths significantly. However, it does result in a slight frequency increase of both the symmetric (2 cm^{-1}) and asymmetric (4 cm^{-1}) C−H stretching vibrations (Table 4). Hydrogen bonding to the NH_3^+ site elongates both C−H bonds more significantly. As a result, the frequencies of the symmetric and asymmetric C−H stretching vibrations downshift by 4 and 6 cm^{-1}, respectively. Two waters added to COO^- and NH_3^+ groups results in an increase in C−H bond lengths and frequency downshifts of the symmetric (4 cm^{-1}) and asymmetric (6 cm^{-1}) stretches.

The MO occupancy listed in Table 5 shows that the water hydrogen bonded to $-NH_3^+$ decreases the electronic density of the N−H bonding orbitals and increases the electronic density of the C−H σ* orbitals. In contrast, water hydrogen bonding to COO^- did not significantly change the C−H bond electronic density.

An additional important insight into the origin of the CH_2 stretching temperature-induced frequency shifts is evident from the CD_3 stretching frequencies of $CD_3-CH_2-ND_2$ and CD_3-CH_2-COOD. As shown above, the CD_3 group, which is not directly connected to the amine or carboxyl, does not show any temperature-induced frequency shifts but does show a significant dependence on the amine and carboxyl group ionization state. Thus, we conclude that the temperature dependence results from some inductive interaction through σ-bonds.

Our calculations show that water hydrogen bonding to the donor ($-NH_3^+$) group downshifts CH_2 stretching frequencies, whereas water hydrogen bonding to the acceptor group ($-COO^-$) upshifts CH_2 stretches. The deprotonated amine ($-NH_2$) and the protonated carboxyl ($-COOH$) can serve as both hydrogen-bond donors and acceptors. Thus, the temperature-induced frequency shift of the CH_2 stretches of gly in solution depends on interplay of different hydrogen-bonding patterns. However, our experimental and theoretical results show that at the pH values close to neutral, hydrogen bonding to the gly $-NH_3^+$ group has dominant effect on the CH_2 stretching frequencies.

CH_2 Stretching Frequency Splitting Monitors Gly Nonplanarity. The splitting between $\nu_s CH_2$ and $\nu_{as} CH_2$ stretching vibrational frequencies should depend less on environment than the frequencies themselves because the splitting depends mostly on C−H bond nonequivalence which depends upon the gly conformation. The actual doublet frequencies can depend on the dielectric constant of the medium, hydrogen bonding to the amine/carboxyl groups, etc. Such environmental factors will likely shift the frequencies of the symmetric and asymmetric stretches in the same direction without significantly changing

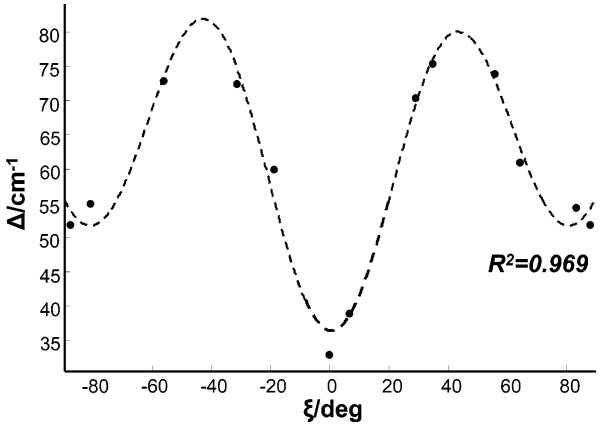

Figure 8. Calculated ξ angular dependence of frequency splitting of the gly CH_2 stretching. The dots represent calculated data points, and the dashed line is the Fourier fit to the calculated results. $\Delta(\xi) = 60 - 10.6\cos(0.04\xi) - 4.3\sin(0.04\xi) - 21.3\cos(0.08\xi) - 3.6\sin(0.08\xi)$.

the splitting between them. This makes the splitting a more reliable probe for gly conformational analysis.

For the planar Gly·HCl molecules the calculated and observed splittings between the $\nu_{as}CH_2$ and ν_sCH_2 vibrations are essentially identical at $\Delta \sim 33$ cm^{-1}. For gly nitrate, Gly·HNO_3, the $\xi \sim 21°$ deviation from planarity results in $\Delta_{Gly\cdot HNO3\ cryst} = 62$ cm^{-1} (Figure 2), whereas the calculated $\xi = 21°$ splitting is $\Delta_{21°,calc} \sim 56$ cm^{-1}. For TGS, the splitting between $\nu_{as}CH_2$ and ν_sCH_2 of the more intense doublet (2982 and 3017 cm^{-1}) corresponding to the almost planar gly pair is $\Delta_{TGS,planar} \sim 35$ cm^{-1}, which again is very close to the calculated value. In contrast for bent gly the observed value is $\Delta_{TGS,bent} \sim 45$ cm^{-1} compared to a calculated $\Delta_{\xi=19°,calculated} = 53$ cm^{-1}. Thus, the splitting between the $\nu_{as}CH_2$ and ν_sCH_2 stretching frequencies definitely depends upon the relative orientations of the CH_2 and carboxylic groups. The small deviations between calculated and measured CH_2 frequency splitting values in crystals may result from crystal packing forces which distort the gly molecules.

As we have shown both experimentally (Figure 2) and theoretically (Figure 7A), the frequency splitting between symmetrical and asymmetrical components of CH_2 stretching depends on the value of ξ angle. Therefore, the frequency splitting (Δ) measured experimentally can be used to determine the ξ angle defined by the gly conformation. Figure 8 shows the frequency splitting calculated for gly conformers versus the ξ angle.

This correlation describes the frequency splitting change which results from the nonplanarity of gly, when the amide group is protonated and the nitrogen lone pair does not affect the CH_2 stretching frequencies.

Conformational Preferences of Gly in Solution. Figure 9 shows Raman spectra of 2,2,2-d_3-ethylamine and gly in solution at pD = 13.3. Two staggered conformations—gauche and anti—are populated in solution at room temperature which differ by a rotation about the C−N bond in ethylamine. In the gauche conformation the nitrogen lone pair is trans to a C−H bond which results in elongation of the trans C−H bond due to electron delocalization from the nitrogen lone pair to the C−H antibonding σ^* orbital which significantly downshifts the C−H stretching frequency by ~100 cm^{-1} to ~2885 cm^{-1}. The other C−H bond is slightly upshifted. Thus, the two most intense, most separated bands at ~2885 and ~2971 cm^{-1} correspond to the uncoupled CH stretches of the gauche conformation of ethylamine. Interaction of the C−H bonds with the lone pair in the anti conformer modestly downshifts both CH stretching

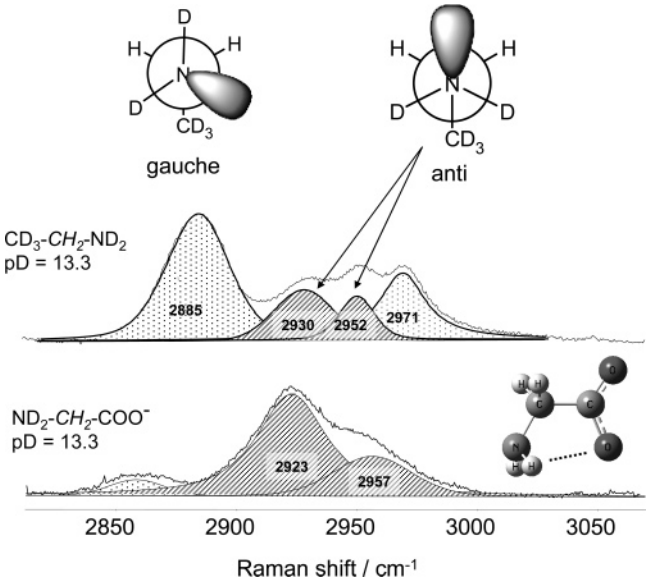

Figure 9. Fitted Raman spectrum (CH_2 stretching region) of the $CD_3-CH_2-ND_2$ and $ND_2-CH_2-COO^-$ solutions in D_2O at pD = 13.3.

vibrations without increasing the frequency splitting between the symmetric and asymmetric components. Thus, the two bands at ~2930 cm^{-1} and 2952 cm^{-1} are ν_sCH_2 and $\nu_{as}CH_2$ of *anti*-ethylamine. Assuming that the areas of the bands are proportional to the population of the ethylamine rotamers in D_2O allows us to calculate that the population of gauche conformers is ~71% and the anti conformer is ~29%. This distribution agrees well with that for *n*-propylamine in the gas phase as determined from the NH_2 wagging and torsion bands in the IR spectra.[47]

In contrast to ethylamine, gly$^-$ shows only two bands at ~2923 (ν_sCH_2) and 2957 cm^{-1} ($\nu_{as}CH_2$), with frequencies similar to those for the anti conformation of 2,2,2-d_3-ethylamine. This indicates that the *anti*-gly$^-$ conformer dominates high pD solutions. This anti conformational preference of gly$^-$ in solution may result from bifurcated intramolecular hydrogen bonding between the amine group hydrogens and the carboxylic group oxygen (Figure 9) Such a hydrogen bond was shown to stabilize gas-phase gly conformations[48,49] and gly molecules in inert gas matrixes at low temperatures.[50] Hyperconjugation could also contribute to the increased stability of the gly anti conformation.[51]

Conclusions

We examined the dependence of the CH_2 stretching frequencies of gly, 2,2,2-d_3-ethylamine, and 3,3,3-d_3-propionic acid on conformation, pD, and temperature by means of Raman spectroscopy (488 nm excitation) and DFT calculations.

Experimental data show a large dependence of the CH_2 stretching frequencies on the ionization state of the amine group. We theoretically demonstrate that the high sensitivity of the ν_sCH_2 and $\nu_{as}CH_2$ frequencies on the orientation and ionization state of the amine group results from a negative hyperconjugation between the nitrogen lone pair and antibonding C−H orbitals. This effect is maximal when a C−H bond is trans to the lone pair.

The C−H stretching frequency dependence on the carboxyl group ionization state is small; however, carboxyl group orientation affects the CH_2 symmetric and asymmetric stretching frequencies as well as their frequency splitting. The magnitude of frequency splitting between the ν_sCH_2 and $\nu_{as}CH_2$ depends

on the relative orientation of the CH_2 and $COOH/COO^-$ groups. The calculated conformational dependence of the CH_2 stretches frequency splitting ($\nu_{as}CH_2 - \nu_sCH_2$) agrees well with the experimental data obtained from gly crystals.

According to our experimental observations and theoretical calculations, the temperature dependence of the ν_sCH_2 and ν_{as}-CH_2 of gly in solution is due to the change in hydrogen-bonding strength of the amine and carboxyl groups to water. This effect has an inductive mechanism and occurs only for the CH_2 directly connected to amine/carboxyl groups by a σ-bond. The magnitude of the frequency shifts varies with the ionization states of amine/carboxyl groups. At pD values close to neutral, hydrogen bonding to the protonated amine group ($-NH_3^+$) is likely to dominate the temperature dependence of the CH_2 stretches of gly.

CD_3 stretching of the deuterated methyl of 2,2,2-d_3-ethylamine and 3,3,3-d_3-propionic acid shows a significant dependence on the ionization state of the amine and carboxylic groups even though the CD_3 group is separated by a CH_2 group. It appears that the delocalization of the electron density from the amine and carboxyl groups to the CH/CD bonds occurs "through space" and requires interacting groups to be spatially close, but not necessarily linked by a covalent bond. Our results indicate that in D_2O at high pD gly is predominantly in an anti conformation in contrast to 2,2,2-d_3-ethylamine which exists in both anti and gauche conformers.

Acknowledgment. This work was supported by NIH Grant GM8RO1EB002053.

References and Notes

(1) Huang, C.-Y.; Getahun, Z.; Wang, T.; DeGrado, W. F.; Gai, F. *J. Am. Chem. Soc.* **2001**, *123*, 12111−12112.
(2) Hamm, P.; Hochstrasser, R. M. *Pract. Spectrosc.* **2001**, *26*, 273−347.
(3) Lednev, I. K.; Karnoup, A. S.; Sparrow, M. C.; Asher, S. A. *J. Am. Chem. Soc.* **2001**, *123*, 2388−2392.
(4) Mikhonin, A. V.; Asher, S. A.; Bykov, S. V.; Murza, A. *J. Phys. Chem. B* **2007**, *111*, 3280−3292.
(5) Brewer, S. H.; Song, B.; Raleigh, D. P.; Dyer, R. B. *Biochemistry* **2007**, *46*, 3279−3285.
(6) Shi, Z.; Chen, K.; Liu, Z.; Kallenbach, N. R. *Chem. Rev.* **2006**, *106*, 1877−1897.
(7) Chi, Z.; Chen, X. G.; Holtz, J. S. W.; Asher, S. A. *Biochemistry* **1998**, *37*, 2854−2864.
(8) Mikhonin, A. V.; Bykov, S. V.; Myshakina, N. S.; Asher, S. A. *J. Phys. Chem. B* **2006**, *110*, 1928−1943.
(9) Mirkin, N. G.; Krimm, S. *J. Phys. Chem. A* **2004**, *108*, 10923−10924.
(10) Mirkin, N. G.; Krimm, S. *J. Phys. Chem. A* **2007**, *111*, 5300−5303.
(11) Ohno, K.; Nomura, S.-I.; Yoshida, H.; Matsuura, H. *Spectrochim. Acta, Part A* **1999**, *55A*, 2231−2246.
(12) Longhi, G.; Zerbi, G.; Paterlini, G.; Ricard, L.; Abbate, S. *Carbohydr. Res.* **1987**, *161*, 1−22.
(13) McKean, D. C. *J. Mol. Struct.* **1976**, *34*, 181−185.
(14) McKean, D. C.; Duncan, J. L.; Batt, L. *Spectrochim. Acta, Part A* **1973**, *29*, 1037−1049.
(15) Thomas, H. D.; Chen, K.; Allinger, N. L. *J. Am. Chem. Soc.* **1994**, *116*, 5887−5897.
(16) McKean, D. C. *Chem. Soc. Rev.* **1978**, *7*, 399−422.
(17) Bellamy, L. J. *Advances in Infrared Group Frequencies, Vol. 2: The Infrared Spectra of Complex Molecules*, 2nd ed.; Chapman and Hall: London, 1980.
(18) Krieger, F.; Moeglich, A.; Kiefhaber, T. *J. Am. Chem. Soc.* **2005**, *127*, 3346−3352.
(19) Vertessy, B. G. *Proteins: Struct., Funct., Genet.* **1997**, *28*, 568−579.
(20) Kohn, W.; Sham, L. J. *Phys. Rev.* **1965**, *137*, 1697−1705.
(21) Parr, R. G.; Yang, W. *Density-Functional Theory of Atoms and Molecules*; Oxford University Press: Oxford, 1989.
(22) Hohenberg, P.; Kohn, W. *Phys. Rev.* **1964**, *136*, B864.
(23) Becke, A. D. *J. Chem. Phys.* **1993**, *98*, 5648−5652.
(24) Lee, C.; Yang, W.; Parr, R. G. *Phys. Rev. B: Condens. Matter Mater. Phys.* **1988**, *37*, 785−789.
(25) Miehlich, B.; Savin, A.; Stoll, H.; Preuss, H. *Chem. Phys. Lett.* **1989**, *157*, 200−206.
(26) Irikura, K. K.; Johnson, R. D., III; Kacker, R. N. *J. Phys. Chem. A* **2005**, *109*, 8430−8437.
(27) Halls, M. D.; Velkovski, J.; Schlegel, H. B. *Theor. Chem. Acc.* **2001**, *105*, 413−421.
(28) Miertus, S.; Scrocco, E.; Tomasi, J. *Chem. Phys.* **1981**, *55*, 117−129.
(29) Cossi, M.; Barone, V.; Mennucci, B.; Tomasi, J. *Chem. Phys. Lett.* **1998**, *286*, 253−260.
(30) Mennucci, B.; Tomasi, J. *J. Chem. Phys.* **1997**, *106*, 5151−5158.
(31) Bader, R. F. W. *Atoms in Molecules: A Quantum Theory*; Oxford University Press: Oxford, 1990.
(32) Cioslowski, J.; Mixon, S. T. *J. Am. Chem. Soc.* **1991**, *113*, 4142−4145.
(33) Cioslowski, J. *Chem. Phys. Lett.* **1992**, *194*, 73−78.
(34) Frisch, M. J.; Trucks, G. W.; Schlegel, H. B.; Scuseria, G. E.; Robb, M. A.; Cheeseman, J. R.; Montgomery, J. A., Jr.; Vreven, T.; Kudin, K. N.; Burant, J. C.; Millam, J. M.; Iyengar, S. S.; Tomasi, J.; Barone, V.; Mennucci, B.; Cossi, M.; Scalmani, G.; Rega, N.; Petersson, G. A.; Nakatsuji, H.; Hada, M.; Ehara, M.; Toyota, K.; Fukuda, R.; Hasegawa, J.; Ishida, M.; Nakajima, T.; Honda, Y.; Kitao, O.; Nakai, H.; Klene, M.; Li, X.; Knox, J. E.; Hratchian, H. P.; Cross, J. B.; Bakken, V.; Adamo, C.; Jaramillo, J.; Gomperts, R.; Stratmann, R. E.; Yazyev, O.; Austin, A. J.; Cammi, R.; Pomelli, C.; Ochterski, J. W.; Ayala, P. Y.; Morokuma, K.; Voth, G. A.; Salvador, P.; Dannenberg, J. J.; Zakrzewski, V. G.; Dapprich, S.; Daniels, A. D.; Strain, M. C.; Farkas, O.; Malick, D. K.; Rabuck, A. D.; Raghavachari, K.; Foresman, J. B.; Ortiz, J. V.; Cui, Q.; Baboul, A. G.; Clifford, S.; Cioslowski, J.; Stefanov, B. B.; Liu, G.; Liashenko, A.; Piskorz, P.; Komaromi, I.; Martin, R. L.; Fox, D. J.; Keith, T.; Al-Laham, M. A.; Peng, C. Y.; Nanayakkara, A.; Challacombe, M.; Gill, P. M. W.; Johnson, B.; Chen, W.; Wong, M. W.; Gonzalez, C.; Pople, J. A. *Gaussian 03*, revision C.01 ed.; Gaussian, Inc.: Wallingford, CT, 2004.
(35) Martin, J. M. L.; Alsenoy, C. V. *GAR2PED*; University of Antwerpen: Antwerpen, Belgium, 1995.
(36) Al-Karaghouli, A. R.; Cole, F. E.; Lehmann, M. S.; Miskell, C. F.; Verbist, J. J.; Koetzle, T. F. *J. Chem. Phys.* **1975**, *63*, 1360−1366.
(37) Narayanan, P.; Venkataraman, S. *J. Cryst. Mol. Struct.* **1975**, *5*, 15−26.
(38) Itoh, K.; Mitsui, T. *Ferroelectrics* **1973**, *5*, 235−251.
(39) Manocha, A. S.; Tuazon, E. C.; Fateley, W. G. *J. Phys. Chem.* **1974**, *78*, 803−807.
(40) Robertson, A. H. J.; McQuillan, G. P.; McKean, D. C. *J. Chem. Soc., Dalton Trans.* **1995**, 3941−3954.
(41) Ho, B. K.; Brasseur, R. *BMC Struct. Biol.* **2005**, *5*, 14.
(42) Lii, J.-H.; Chen, K.-H.; Allinger, N. L. *J. Phys. Chem. A* **2004**, *108*, 3006−3015.
(43) Henbest, H. B.; Meakins, G. D.; Nicholls, B.; Wagland, A. A. *J. Chem. Soc.* **1957**, 1462−1464.
(44) Hamlow, H. P.; Okuda, S.; Nakagawa, N. *Tetrahedron Lett.* **1964**, 2553−2559.
(45) McKean, D. C.; Ellis, I. A. *J. Mol. Struct.* **1975**, *29*, 81−96.
(46) Bellamy, L. J.; Mayo, D. W. *J. Phys. Chem.* **1976**, *80*, 1217−1220.
(47) Sato, N.; Hamada, Y.; Tsuboi, M. *Spectrochim. Acta, Part A* **1987**, *43A*, 943−954.
(48) Hu, C. H.; Shen, M.; Schaefer, H. F., III. *J. Am. Chem. Soc.* **1993**, *115*, 2923−2929.
(49) Jensen, J. H.; Gordon, M. S. *J. Am. Chem. Soc.* **1991**, *113*, 7917−7924.
(50) Ivanov, A. Y.; Sheina, G.; Blagoi, Y. P. *Spectrochim. Acta, Part A* **1999**, *55A*, 219−228.
(51) Wang, W.; Pu, X.; Zheng, W.; Wong, N.-B.; Tian, A. *Chem. Phys. Lett.* **2003**, *370*, 147−153.